Cell, Vol. 123, 195–205, October 21, 2005, Copyright ©2005 by Elsevier Inc. DOI 10.1016/j.cell.2005.10.001

Theory

A Structure-Based Model for the Synthesis and Hydrolysis of ATP by F_1-ATPase

Yi Qin Gao,[1,3] Wei Yang,[1,3] and Martin Karplus[1,2,*]
[1]Department of Chemistry and Chemical Biology
Harvard University
Cambridge, Massachusetts 02138
[2]Laboratoire de Chimie Biophysique, ISIS
Université Louis Pasteur
67000 Strasbourg
France

Many essential functions of living cells are performed by nanoscale protein motors. The best characterized of these is F_oF_1-ATP synthase, the smallest rotary motor. This rotary motor catalyzes the synthesis of ATP with high efficiency under conditions where the reactants (ADP, $H_2PO_4^-$) and the product (ATP) are present in the cell at similar concentrations. We present a detailed structure-based kinetic model for the mechanism of action of F_1-ATPase and demonstrate the role of different protein conformations for substrate binding during ATP synthesis and ATP hydrolysis. The model shows that the pathway for ATP hydrolysis is not simply the pathway for ATP synthesis in reverse. The findings of the model also explain why the cellular concentration of ATP does not inhibit ATP synthesis.

Introduction

The motor enzyme F_oF_1-ATP synthase of mitochondria uses the proton-motive force across the mitochondrial membranes to make ATP from ADP and P_i ($H_2PO_4^-$) (Boyer, 1997; Abrahams et al., 1994; Senior et al., 2002; Karplus and Gao, 2004). It does so under cellular conditions that favor the hydrolysis reaction by a factor of 2×10^5. In fact, as a result of the activity of the F_oF_1-ATP synthase, the concentration ratio (ATP:ADP/P_i) is close to unity in mitochondria (Karplus and Gao, 2004; Nakamoto et al., 2000). This remarkable property is based on the essential difference between an ordinary enzyme, which increases the rate of reaction without shifting the equilibrium, and a catalytic motor (Alberts, 1998) like F_oF_1-ATP synthase, which can drive a reaction away from equilibrium by harnessing an external force. Given that a sedentary adult synthesizes and uses about 40 kg of ATP per day (Voet and Voet, 1995), an understanding of the detailed mechanism of F_oF_1-ATP synthase is essential for a molecular explanation of the biology of living cells.

F_oF_1-ATP synthase is composed of two domains (Figure 1): a transmembrane portion (F_o), the rotation of which is induced by a proton gradient, and a globular catalytic moiety (F_1) that synthesizes and hydrolyzes ATP. In this article, we focus on the F_1-ATPase moiety, for which high-resolution structures are available (Abrahams et al., 1994; Gibbons et al., 2000; Braig et al., 2000; Menz et al., 2001; Kagawa et al., 2004). F_1-ATPase can synthesize, as well as hydrolyze, ATP. ATP synthesis has been demonstrated recently by applying an external torque to the γ subunit, causing it to rotate in the reverse direction from that observed during ATP hydrolysis (Itoh et al., 2004). Thus, the primary function of the proton-motive force acting on F_oF_1-ATP synthase is to provide the torque required to rotate the γ subunit in the direction for ATP synthesis.

F_1-ATPase has three α and three β subunits arranged in alternation around the γ subunit, which has a globular base and an extended coiled-coil domain (Abrahams et al., 1994) (Figure 1). All of the α and β subunits bind nucleotides, but only the three β subunits are catalytically active. The crystal structures of F_1-ATPase provide views of distinct conformational states of the catalytic β subunits (Abrahams et al., 1994; Braig et al., 2000; Menz et al., 2001; Kagawa et al., 2004). The centrally located and asymmetric γ subunit forms a shaft, and it has been proposed that its orientation determines the conformations of the β subunits. The original crystal structure (Abrahams et al., 1994) of F_1-ATPase from bovine heart mitochondria led to the identification of three conformations of the β subunit: β_E (empty), β_{TP} (ATP analog bound), and β_{DP} (ADP bound). In a more recent high-resolution crystal structure (Menz et al., 2001), the β_{TP} and β_{DP} subunits contain an ATP analog (ADP plus AlF_4^-) and the third catalytic subunit has a half-closed conformation, called β_{HC}, containing ADP plus SO_4^- (an analog of P_i). The open β_E and half-closed β_{HC} conformations of the third β subunit are both very different from those of the β_{TP} and β_{DP} subunits, which are both closed and very similar to each other in all structures. Specifically, the β_{HC} conformation is between the "open" β_E conformation, in which the interaction between β strands 3 and 7 is disrupted, and the "closed" β_{TP} and β_{DP} conformations (Figure 2), in which the nucleotide binding domain and α-helical domain have rotated toward each other by 30° with respect to their positions in β_E (Abrahams et al., 1994).

From his insightful analysis of kinetic data, in advance of detailed structural information, Paul Boyer proposed a "binding change mechanism" by which rotary catalysis could operate (Boyer, 1993). In a modern interpretation of the mechanism, which differs in detail from Boyer's original proposal, ATP synthesis proceeds by the cyclical conversion of each of the β subunits from an "open" state that binds to nucleotide only weakly to a "tight" state that has highest affinity for ATP and finally to a "loose" state, which has a lower affinity for ATP and from which ATP can be released. The first crystal structure (Abrahams et al., 1994) clearly supported the general features of the binding change mechanism, as did single-molecule experiments (Noji et al., 1997; Yasuda et al., 1998, 2001). Researchers were reluctant to accept the rotary mechanism until its explicit visualization (Noji et al., 1997), but it is now generally accepted and forms the conceptual basis of the quantitative model we present here.

Given the remarkable properties of F_1-ATPase, this rotary-motor enzyme has been the subject of many ex-

*Correspondence: marci@tammy.harvard.edu
[3]These authors contributed equally to this work.

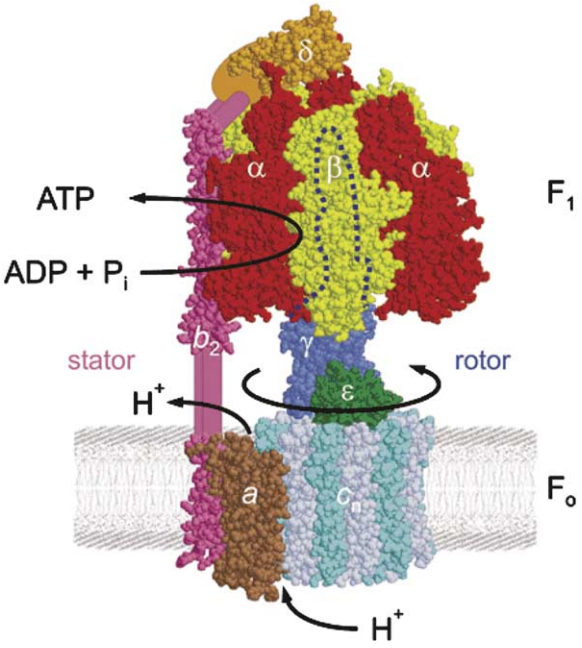

Figure 1. Structural Model of F_oF_1-ATP Synthase

The figure is from Senior et al. (2002) with permission of the author. The F_1 portion is based on the crystal structure determined by Gibbons et al. (2000), and the F_o portion is based on NMR and mutation data obtained by Rastogi and Girvin (1999). The three conformations of the β subunits in the 1BMF crystal structure (Abrahams et al., 1994) (E_1 in this paper) are called β_E (empty), β_{TP} (bound with AMP-PNP), and β_{DP} (bound with ADP), and the three conformations of the β subunits in the 1H8E crystal structure (Menz et al., 2001) (E_2 in this paper) are called β_{HC} (bound with ADP/SO_4^{2-}), β_{TP} (bound with ADP/AlF_4^-), and β_{DP} (bound with ADP/AlF_4^-).

perimental studies. Nevertheless, a detailed understanding of the mechanism by which it carries out its functions is not available. Several pictorial models of the mechanism of F_1-ATPase hydrolysis have been proposed (Boyer, 1997; Menz et al., 2001; Weber and Senior, 1997; Allison, 1998), but none of them provide a consistent and comprehensive picture of how the F_1-ATPase operates during both ATP hydrolysis and ATP synthesis. This is due mostly to the lack of a quantitative description of how the thermodynamics and kinetics of the enzyme are related to the structural data. Essential elements for developing such a mechanism have been missing. However, recent molecular dynamics simulations have supplied the "missing link" between the high-resolution crystal structure of F_1-ATPase and the measurements in solution and of single molecules.

On the basis of these results, we can now formulate a consistent structure-based model for both ATP synthesis and hydrolysis by F_1-ATPase. In developing this model, we have sought to answer a number of essential questions, which are listed below. We focus here on the primary function of the F_1-ATPase motor—that is, ATP synthesis—although a corresponding model for hydrolysis is also given in the paper. For each question, we indicate in general terms how it is resolved by our analysis. More complete explanations are provided in the Results and Discussion.

1. ***How Does Rotation of the γ Shaft Induced Either by the Proton-Motive Force (Boyer, 1997) or an External Force (Itoh et al., 2004) Alter the Conformations of the Catalytic Subunits?***

The mechanism involved has been elucidated by molecular dynamics simulations (Ma et al., 2002; Böckmann and Grubmüller, 2002) and normal mode calculations of F_1-ATPase (Cui et al., 2004; Sun et al., 2003).

2. What Is the Binding Affinity of Each Structurally Defined Binding Site?

Specifically, what is the relationship between the measured solution affinities for ATP and ADP, P_i, and the binding sites in the different conformations of the catalytic subunits observed in the X-ray structures? Answering this question is critical to generating a consistent model for the function of F_1-ATPase. The answer determines the role of the different protein conformations in the synthesis and hydrolysis of ATP. Because

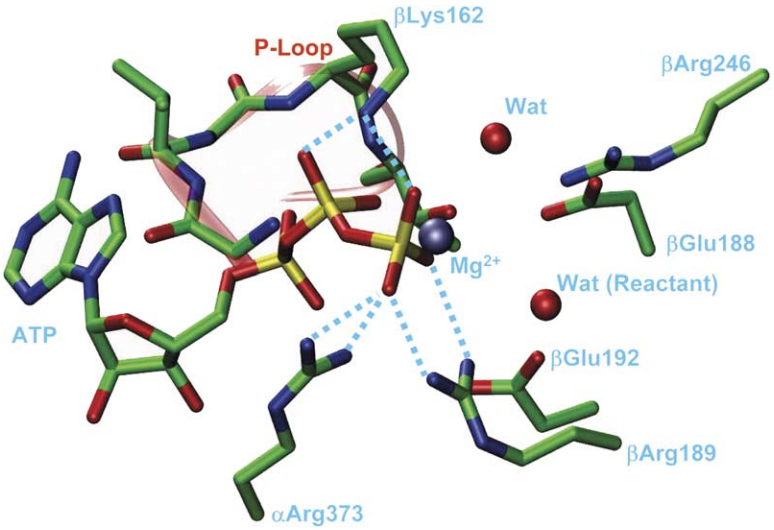

Figure 2. The Structure of the β_{DP} Site with Bound ATP

For clarity, only the most important residues discussed in the text are shown. The structure is based on a crystal structure (1H8E) with ADP and $AlF4^-$ in the binding site. To obtain the structure illustrated, the ATP was created by overlapping the corresponding portion with ADP, and the γ-phosphate was superimposed on the Al atom. The system with the ATP ligand modeled into the active site was allowed to relax by a molecular dynamics simulation and is close to the original crystal structure.

these sites exist in a single structure, measurement of their individual binding affinities has not been possible. This is in contrast to most other motor proteins, such as myosin, in which separate structures with different affinities exist in solution and in crystals. Moreover, the β_{TP} and β_{DP} sites, which are bound with ligands in all structures, have very similar conformations. Recently, the missing link between the experimental solution measurement and X-ray structures has been obtained by the use of free-energy simulations (Yang et al., 2003). The results described in this paper provide the thermodynamic basis for the structure-based model for the synthesis and hydrolysis of ATP by F_1-ATPase.

3. What Is the Mechanism by which F_1-ATPase Synthesizes ATP from ADP and Pi against a Strong Thermodynamic Driving Force Biased toward Hydrolysis?

Although the essential concept is contained in the binding change mechanism of Boyer, an unresolved issue has been how the rotation of the γ subunit is coupled to the different conformations and binding affinities of the catalytic β subunits. This is now understood, given the answers to questions 1 and 2, and is described in detail here.

4. How Does the Enzyme Avoid Being Inhibited by ATP during ATP Synthesis When Its Concentration Is Essentially Equal to that of ADP and P_i, as It Is in the Mitochondria? How Is the Enzyme Optimized for Both ATP Synthesis and Hydrolysis as the Only Bidirectional Protein Machine in the Cell?

The thermodynamic understanding of F_1-ATPase allows us to construct a kinetic model, which answers these questions. The important realization for explaining the bidirectional functionality of F_1-ATPase is that synthesis is not the exact inverse of hydrolysis, in accord with a prescient suggestion of Senior et al. (2002). Different catalytic subunits are involved in substrate binding and release in synthesis and hydrolysis. This is codified in the structure-based kinetic model, which has the E_1E_2 mechanism (DeMeis and Vianna, 1979) as one of its essential elements. In the current realization of the E_1E_2 mechanism, two major protein conformations are involved, one for reactant binding and the other for product release. ADP/P_i binding in synthesis and release during hydrolysis involves primarily the "half-closed" β_{HC} site in the E_2 conformation; ATP release during synthesis and binding during hydrolysis involves primarily the open β_E site in the E_1 conformation. The resulting kinetic model not only provides an interpretation of the available kinetic data but predicts new results. It also indicates how the activity of F_1-ATPase is regulated in the cell as a function of the physiological concentrations of ATP, ADP, and P_i.

5. What Is the Chemical Occupancy of Each Structurally Defined Binding Site during ATP Synthesis and Hydrolysis?

The answer resolves whether synthesis and hydrolysis operate through a bisite or trisite mechanism, a question that continues to be debated. By a bisite mechanism (Boyer, 1993), we mean that, at any stage of ATP hydrolysis or synthesis, the occupation of only two catalytic sites but not the third is required, whereas a trisite mechanism (Senior et al., 2002) requires all three sites to be occupied for the maximal rate of enzyme function. The analysis demonstrates that a trisite mechanism is operative when F_1-ATPase is working optimally and elucidates how the cooperativity among the catalytic subunits is achieved. The negative cooperativity of ATP and ADP binding to the catalytic sites plays an essential role in generating the driving force for the rotation of the γ subunit during ATP hydrolysis. In turn, the rotation of the γ subunit leads to positive cooperativity during catalysis. We note that rotary catalysis leads to an increase in the observed hydrolysis rate by a factor of up to 5×10^5 relative to unisite catalysis (Boyer, 1993, 1997; Gao et al., 2003).

6. How Are the Chemical Reactions (ATP Synthesis and Hydrolysis) Modulated by the Essential Residues in the Binding Pocket?

Specifically, how is hydrolysis of ATP prevented when the affinity of the enzyme for ATP is reduced after its synthesis, permitting release of ATP? From molecular dynamics simulations, we show that the positions of the catalytic residues change during the reaction cycle and that they are no longer in a position to accelerate the reaction when ATP is released.

Results and Discussion

Rotational Mechanism for Chemomechanical Coupling (Questions 1 and 3)

Two molecular dynamics simulations (Ma et al., 2002; Böckmann and Grubmüller, 2002) have provided important insights into the mechanism of F_1-ATPase action. Both calculations were performed with rotation of the γ subunit enforced in the direction predicted for synthesis (see Itoh et al. [2004] and Diez et al. [2004] for an experimental confirmation of this assumption). The timescale for one rotation of the γ shaft is in the microsecond-to-millisecond range (Kinosita et al., 2004) and is therefore not directly accessible to the nanosecond timescales probed by standard molecular dynamics simulations. To overcome this problem, the conformational transitions in F_1-ATPase were obtained by molecular dynamics simulations in the presence of biasing forces, which were applied to either the γ subunit alone or the entire structure in a procedure that drives the system from one state to the other without explicitly constraining the nature of the transition path. The implicit assumption in such studies is that meaningful information concerning the mechanism can be obtained even though the time scale of the forced rotational transition of the γ subunit is several orders of magnitude faster than the actual rotation rate.

The simulation results demonstrate how the rotation of the γ subunit induces the structural changes in the catalytic β subunits and explain why there is much less movement in the catalytically inactive α subunits that are bound to ligand. Both van der Waals (steric) and electrostatic interactions contribute to the coupling between the β and the γ subunits. The dominant electrostatic interactions occur between positive residues of both the coiled-coil portion and the globular region of the γ subunit (the "ionic track") and the negatively charged residues of the β subunits (see Figures 4 and 5 of Ma et al. [2002]). This ionic track leads to a smooth rotation pathway without large jumps in the coupling energy and is likely to contribute to the high efficiency

of the chemomechanical energy transduction. The importance of some of the residues involved has been explored by mutation experiments (for a recent study, which reviews some of the earlier data, see Greene and Frasch [2003]). The simulations show how the rotation of the γ subunit induces the opening motion of the β subunits. In contrast, the closing motion of the β subunits appears to be spontaneous, once ligand is bound to the active site and there are no steric interactions caused by the γ subunit. This has been confirmed recently for an isolated β subunit in solution by nuclear magnetic resonance (NMR) (Yagi et al., 2004). Interestingly, the conformational changes observed in the β subunits have been shown to correspond to their lowest frequency normal modes (Cui et al., 2004). This implies that the structure of the protein is designed by evolution such that the motions required for its function can take place with a low energy cost.

Identification of Solution Binding Affinities with β Subunit Conformations (Questions 2 and 3)

An essential element of the mechanism of F_1-ATPase action is the standard free-energy difference between ATP, H_2O, and ADP/P_i at the catalytic sites associated with the different β subunit conformations. Four different binding constants for ATP have been measured for F_1-ATPase in solution. The values for the *E. coli* enzyme are 0.2 nM, 2 μM, 25 μM, and 5 mM, respectively (Gao et al., 2003). It is generally agreed that the open (β_E) and half-closed (β_{HC}) subunits have the two weakest binding sites and that the two other subunits (β_{TP} and β_{DP}) contain the tightest site and the second highest affinity site. To determine the role played by each of the β subunit conformations in the rotary-catalysis mechanism of F_1-ATPase, it was essential to resolve the uncertainties concerning their binding affinities—that is, to make a connection (the missing link) between the microscopic (structural) and macroscopic (solution) data. This has been achieved recently (Yang et al., 2003, Gao et al., 2003) by combining free-energy difference simulations with experimental data. The free-energy simulations were used to calculate the standard free-energy change (ΔG^0) of the hydrolysis reaction in the various β subunit sites of the crystal structure. Free-energy simulation techniques have been developed to the stage where they can be used for answering quantitative questions in biomolecular systems (Simonson et al., 2002). In the application of these techniques to F_1-ATPase, statistical errors had to be carefully controlled to obtain reliable results (Yang et al., 2004). The bound ATP/H_2O was calculated as having a free energy similar to that of ADP/P_i in the β_{TP} site (1.5 kcal/mol), whereas the free energy in the β_{DP} site favors ADP/P_i relative to ATP/H_2O by 9 kcal/mol. Experiments have shown that under unisite hydrolysis conditions (that is, at ATP concentrations so low that only one ATP is bound to the enzyme), the free energies of ATP/H_2O and ADP/ P_i in the occupied site are nearly the same. The measured ΔG^0 value is 0.4 kcal/mol in the mitochondrial enzyme and −0.6 in the *E. coli* enzyme. Because unisite hydrolysis is expected to take place in the site that has the highest affinity for ATP, the simulation results can be used to identify the β_{TP} and β_{DP} subunits as the ones with the highest and second highest affinity for ATP, respectively. The β_E site, for which no calculations have been made because of the absence of a bound ligand, is identified as the site with a binding constant of 25 μm (Gao et al., 2003). Free-energy simulation results, based on β_{HC} structure, agree with the values measured when the proton-motive force is present (Nakamoto et al., 2000). This indicates that β_{HC} is responsible for binding of the reactants ADP/P_i during ATP synthesis and release of products ADP/P_i during ATP hydrolysis. Having matched the ATP binding constants with specific β subunit conformations, it was also possible to determine the binding constants for ADP and P_i for each of the β sites. This analysis also relied upon both experimental data and free-energy simulations. A surprising finding was that the strong binding site for ADP/P_i is the β_{DP} site, in contrast to the strong binding site for ATP and H_2O, which is the β_{TP} site (for details, see Gao et al. [2003]).

From these results, it can be shown that there are two major contributions to the driving force (actually a biasing free energy) that rotates the γ subunit when ATP is hydrolyzed by F_1-ATPase (Gao et al., 2003). The first contribution is the increase in the binding free energy of ATP in going from the β_E to the β_{TP} state; this is in agreement with the original model of Wang and Oster (1998). However, the second contribution is a new result; it arises from the fact that, once hydrolysis takes place and ADP/P_i occupies the binding site, the conformation is biased toward β_{DP}.

Subunit Thermodynamics in ATP Synthesis and Hydrolysis

In accordance with the E_1E_2 model, different conformations of the catalytic β subunits serve for substrate binding and product release during ATP synthesis and hydrolysis. Figure 3A shows the thermodynamic properties of the different conformations of the catalytic β subunits involved in the ATP synthesis reaction, which is driven by a clockwise rotation of the γ subunit (see also Figure 4). The corresponding diagram for hydrolysis is shown in Figure 3B. The β_{HC} subunit binds ADP/P_i because ADP/P_i has a lower free energy in the β_{HC} subunit than in solution. Also, the rate of binding is expected to be relatively fast. The value for the ADP "on" constant for *E. coli* F_1-ATPase is about 10^6 $M^{-1}s^{-1}$ (Senior et al., 2002); however, that for P_i is not known. Because the potential of ATP in the β_{HC} site is higher than that in solution (see Figure 3A), there is little interference (inhibition) from ATP binding, even when it is present at a concentration similar to that of ADP/P_i. This is one of the essential elements of the E_1E_2 model. Rotation of the γ subunit by 90°, after ADP and P_i are bound (see Figure 4), transforms β_{HC} into β_{DP}. This conformational change does not induce synthesis because the reaction free energy still strongly favors ADP/P_i (see Figure 3A). A further rotation of 120° changes β_{DP} to β_{TP}, the high-affinity site for ATP. The free energies of bound ATP and ADP/P_i are approximately equal in β_{TP}, and synthesis can begin, but the rate is much slower (0.04 s^{-1} in *E. coli*) than the observed maximal rate (10–100 s^{-1} in *E. coli*) (Senior, 1992). A conformational change is required to shift the equilibrium toward ATP and increase the rate of ATP synthesis. Free-energy simulations (Yang et al., 2003; W.Y., Y.Q.G., S. Boresch, and M.K., unpublished data) suggest that this occurs in a conformation similar to β_{TP} but with local structural

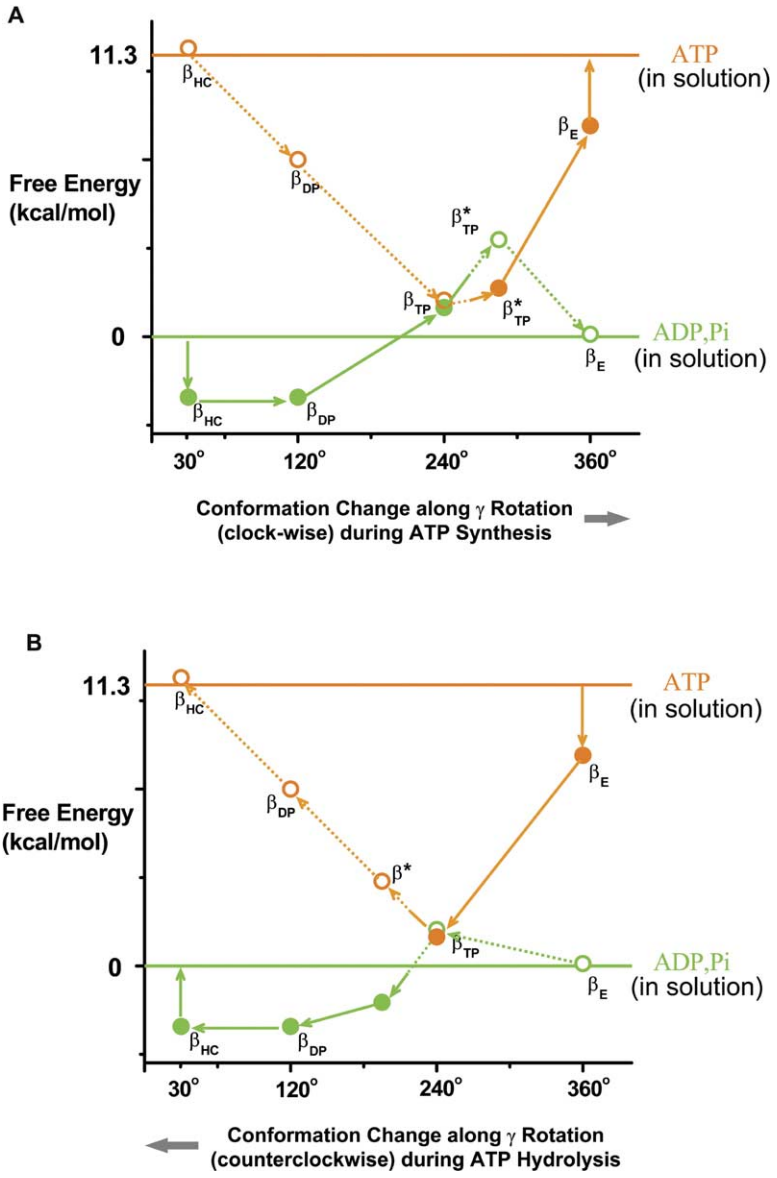

Figure 3. The Changing Chemical Potentials of ATP and ADP/P_i in a β Subunit as a Function of γ Subunit Rotation

A full 360° cycle for a single catalytic subunit is shown (see also Figure 4).

(A) ATP synthesis by the clockwise rotation of the γ subunit. The rotation angle of the γ subunit is indicated on the abscissa, and the corresponding β subunit conformations are shown. In addition to the known structures, an intermediate state, β_{TP}*, favoring ATP, is shown between β_{TP} and β_E sites (see text). Orange is used for ATP and green for ADP/P_i. The thermodynamically favored states are represented by filled circles and the unfavored states by open circles. The dominant transitions are represented by solid arrows and the unimportant ones by dotted arrows. The chemical reaction is indicated by arrows that are half solid green (ADP/P_i) and half solid orange (ATP). The solution state of ATP is represented by an orange line at 11.3 kcal/mol (the potential of ATP relative to ADP/P_i at cellular concentrations; see text), and the solution state of ADP/P_i is represented by a green line, which is set to zero.

(B) ATP hydrolysis, which results in the counterclockwise rotation of the γ subunit. The rotation angle of the γ subunit is indicated on the abscissa, and the corresponding β subunit conformations are shown. In addition to the known structures, an intermediate state, β*, favoring ADP/P_i, is shown to represent where ATP hydrolysis is likely to occur under normal conditions. Orange is used for ATP and green for ADP/P_i. The thermodynamically favored states are represented by filled circles and the unfavored states by open circles; the dominant transitions are represented by solid arrows and the unimportant ones by dotted arrows. The chemical reaction is indicated by arrows that are half solid green (ADP/P_i) and half solid orange (ATP). The solution state of ATP is represented by an orange line at 11.3 kcal/mol (the potential of ATP relative to ADP/P_i at cellular concentrations; see text), and the solution state of ADP/P_i is represented by a green line, which is set to zero.

changes induced by rotation of the γ subunit to about 300°; we refer to this structure, which has not been observed experimentally, as β_{TP}* (Figure 3A). Rotation of the γ subunit to complete the 360° cycle (Figure 3A) creates the β_E site, which binds to ATP less strongly, as required for product release (Antes et al., 2003). As the β_E site is approached, the free energy of ATP becomes higher than that of ADP/P_i. A lower value of the free energy of ATP in the β_E site, relative to that in solution, is required for optimization of hydrolysis, as well as synthesis, because β_E is the binding site for the ATP substrate in hydrolysis, (see Figure 4), as well as the release site for ATP after synthesis. The openness of the β_E site makes the release and binding rate of ATP rapid enough such that it is not rate limiting under normal conditions (see below).

Figure 3B shows the thermodynamics properties of the different conformations of the catalytic β subunits in ATP hydrolysis, which correspond to a counterclockwise rotation of the γ subunit from right (360°) to left (0°) on the abscissa. The β_E site binds ATP more strongly than in solution at the beginning of the rotation cycle, which can prevent the interference of ADP/P_i. Tighter binding of ATP to the β_{TP} site provides a driving force for γ subunit rotation. Rotation of the γ subunit transforms the β_E site in E_1 to the β_{TP} site in E_2. The free energies of bound ATP and ADP/P_i are approximately equal in β_{TP}. Hydrolysis can start at this position, but the rate is much smaller (about ~0.1 s^{-1}, in *E. coli*) than the maximum overall hydrolysis rate (60–80 s^{-1}, in *E. coli*). Another 120° γ subunit rotation, mainly driven by ATP binding to another site, causes the transition $\beta_{TP} \rightarrow \beta_{DP}$, during which the potential for ATP increases and that for ADP/ P_i decreases. Because the β_{DP} site strongly favors ADP/P_i relative to ATP/H_2O and the active-site residues are appropriately positioned for ca-

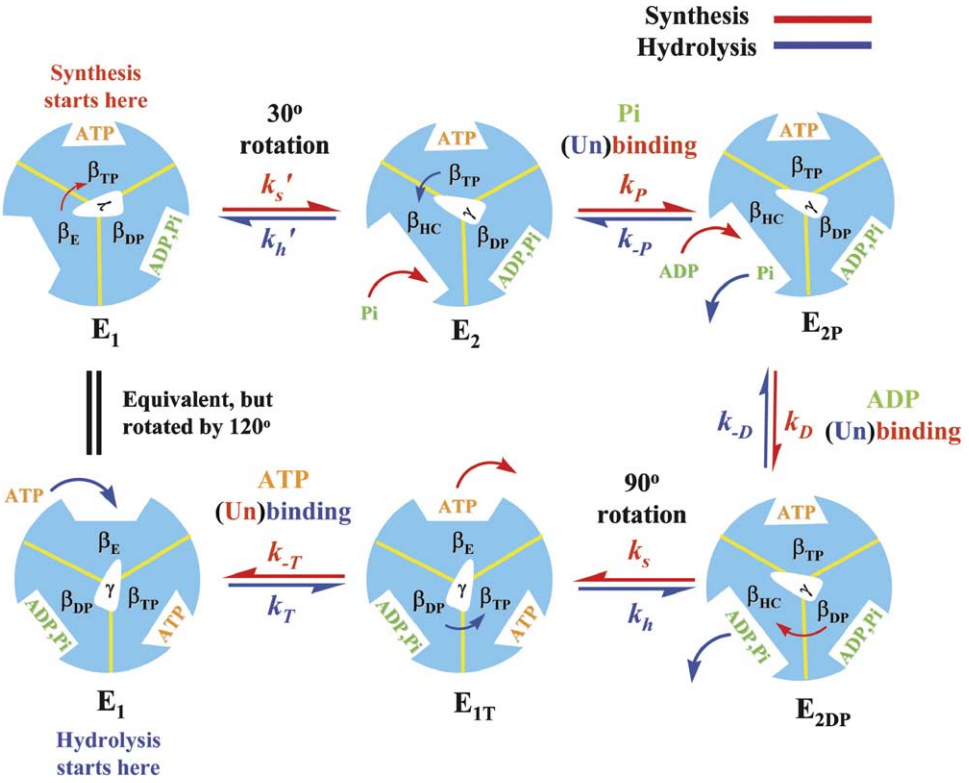

Figure 4. Schematic Diagram Illustrating the Trisite E_1E_2 Model for ATP Synthesis and Hydrolysis by F_1-ATPase

The figure shows a 120° rotation cycle for the molecule, which corresponds to the synthesis or hydrolysis of one ATP. The catalytic binding sites are labeled according to their structural descriptions (β_E, β_{TP}, β_{DP}, and β_{HC}) (Abrahams et al., 1994; Menz et al., 2001) and indicated by various shapes similar to those used in the literature (Braig et al., 2000). ATP is orange and ADP/P_i is green ($P_i = H_2PO_4^-$). The sequence of events for ATP synthesis is shown by red arrows, whereas blue arrows indicate the sequence for ATP hydrolysis. The constant k_x is the binding rate constant for species x at a given binding site, and k_{-x} is the corresponding dissociation rate constant. k_s', k_h', k_s, and k_h are rate constants for the indicated rotations. For hydrolysis, the present scheme is in general agreement with the proposals of Senior et al. (2002) and Kagawa et al. (2004) (see also Supplemental Data).

talysis, hydrolysis is expected to occur during the β_{TP}-to-β_{DP} transition (Gao et al., 2003). Thus, because of the relative binding energies—ATP binding is strongest in the β_{TP} site, whereas ADP/P_i binding is strongest in the β_{DP} site (Gao et al., 2003)—the transition of $\beta_E \rightarrow \beta_{TP}$ involving ATP binding and the transition of $\beta_{TP} \rightarrow \beta_{DP}$ involving ATP hydrolysis contribute most of the energy that drives the rotation of γ subunit (Karplus and Gao, 2004; Gao et al., 2003). In the transition of $\beta_{DP} \rightarrow \beta_{HC}$, the overall binding affinity for ADP/P_i changes moderately, but the ADP binding affinity is lowered by about 3.7 kcal/mol, and the P_i binding affinity is increased by about the same amount. This suggests that ADP is released first, followed by P_i. This unbinding sequence is supported by inhibition measurement (see the Supplemental Data available with this article online). The release of P_i, which, when bound, constrains the system in E_2 (with the β_{HC} conformation), permits a 30° γ subunit rotation to transform the structure to E_1 (with $\beta_{HC} \rightarrow \beta_E$) and complete the 360° cycle (see Figure 3B). The 30° rotation is driven by energy that we suggest is stored in the twisted γ subunit during ATP binding in hydrolysis (W.Y., Y.Q.G., S. Boresch, and M.K., unpublished data). Because of the high binding affinity of the β_{HC} site for P_i, the release of P_i is the rate-limiting step at high ATP concentration; this is a necessary aspect of efficient ATP synthesis, as indicated above.

Model for Complete F_1-ATPase Catalytic Cycle (Questions 3 and 4)

The catalytic cycle for ATP synthesis and hydrolysis by F_1-ATPase is illustrated in Figure 4. Two different conformations of F_1-ATPase participate in the reaction cycle, in formal analogy to the E_1E_2 model (DeMeis and Vianna, 1979). As a result, there are different binding sites for the substrates in ATP synthesis (ADP/P_i) and hydrolysis (ATP) and for the products (ATP and ADP/P_i, respectively). Experimental binding data and free-energy simulations (Yang et al., 2003) suggest that structure E_1 has the subunit conformations β_{TP}, β_{DP}, and β_E (Abrahams et al., 1994), whereas E_2 consists of β_{TP}, β_{DP}, and β_{HC} (Menz et al., 2001) (Figure 1). The two rotation steps (30° and 90°) shown in Figure 4 correspond to those in single-molecule hydrolysis experiments (Yasuda et al., 2001) and are assumed to occur in synthesis. As of yet, there is no direct evidence for this assumption. The ATP synthesis reaction begins with a γ subunit rotation of approximately 30° due to the proton motive force acting on the F_1 moiety through the F_o complex (Diez et al., 2004) or, equivalently, an

external force (Itoh et al., 2004), changing E_1 to E_2 and, most importantly, $\beta_E \rightarrow \beta_{HC}$. (Menz et al., 2001). Binding of the substrates P_i and ADP to the β_{HC} subunit takes place without rotation. Once the substrates are bound, a 90° rotation occurs, which changes E_2 to E_1. ATP synthesis occurs during this step and is followed by product release from β_E. In ATP hydrolysis, the ATP substrate binds to the β_E subunit of E_1 and the hydrolysis products are released from the β_{HC} subunit of E_2. The ATP hydrolysis reaction occurs in a conformation between that of the β_{TP} and β_{DP} sites. The rotation of the γ subunit is produced by the differential binding of ATP and ADP/P_i to the various subunit conformations, as described above (Boyer, 1997; Senior et al., 2002; Karplus and Gao, 2004).

The total free energy of ATP hydrolysis or synthesis can be divided into five components (Figure 4). They are the binding free energy of ATP ($-\Delta G_T = RT\ln(k_T[ATP]/k_{-T})$); two free-energy changes, denoted hereafter as W_1 and W_2, associated with the rotation of the γ subunit; and the free energies associated with release of ADP ($-\Delta G_D = RT\ln(k_{-D}/k_D[ADP])$) and P_i ($-\Delta G_P = RT\ln(k_{-P}/k_P[P_i])$). For definitions of the symbols, see the legend of Figure 4. Because the free-energy components W_1 and W_2 are associated with the γ subunit rotation, they are functions of the external load. The free-energy change for ATP hydrolysis in the absence of an external load can be written as

$$\Delta G_{sol} = W_1 + W_2 + \Delta G_T - \Delta G_D - \Delta G_P, \quad (1)$$

where ΔG_{sol} is the free energy of ATP hydrolysis in solution. At concentrations of 1 M for ATP, ADP, and P_i, ΔG_{sol} = –7.3 kcal/mol (Stryer, 1995), whereas at cellular concentrations, the value is –12.3 kcal/mol for human cells and –11.3 kcal/mol for *E. coli* (Nelson and Cox, 2000). From Figure 4, the rate constants for the rotation of the γ subunit k_h, k_s and k'_h, k'_s are related through the free-energy changes W_1 and W_2, respectively,

$$\frac{k_h}{k_s} = e^{-W_1/k_BT}, \frac{k'_h}{k'_s} = e^{-W_2/k_BT}, \quad (2)$$

where k_B is the Boltzmann constant and T is the temperature. When an external load $F_{ext}(\theta)$ is applied to the system via the γ subunit (as by, for example, the protonmotive force), an additional term has to be introduced into Equation 1. The integration range for the rotation of the γ subunit per ATP hydrolyzed or synthesized is 0° to 120°. In the case of proton transport, $\int_0^{120} F_{ext}(\theta)d(\theta) = n\Delta\mu_{H^+}$, where n is the number of protons transported across the inner membrane of the mitochondrion per ATP hydrolyzed (synthesized) and $\Delta\mu_{H^+}$ is the proton free-energy gradient. The existing experimental data indicate that n = 4 (Senior et al., 2002; Karplus and Gao, 2004), although the exact value is a still a matter of debate. Accordingly, $W = W_1 + W_2$, the total free-energy change corresponding to the elementary step (120° rotation of the γ subunit) in the presence of an external force, can be written as

$$W = W_1 + W_2 = \Delta G_{sol} - \Delta G_T + \Delta G_D + \Delta G_P + \int F_{ext}(\theta)d\theta. \quad (3)$$

Because the concentration dependence $(-\ln[ATP]/[ADP][P_i])$ in ΔG_{sol} cancels exactly with that in ΔG_T, ΔG_D, and ΔG_P, W is independent of the solution concentrations of ATP, ADP, or P_i, as it should be. The binding and dissociation rate constants of the substrates ATP and ADP have been obtained from experimental measurements such as the fluorescence quenching experiments of Weber and Senior (1997) for the *E. coli* system. The rate constants k_h, k_s and k'_h, k'_s represent the rate of rotation of the γ subunit of the F_1-ATPase in Figure 4 and can be measured by single-molecule experiments (Yasuda et al., 2001).

Kinetic Analysis of ATP Synthesis and Hydrolysis by F_1-ATPase (Questions 4 and 5)

In the following, we use the model given in Figure 4 to estimate important kinetic properties of F_1-ATPase, including the ATP, ADP, and P_i concentration dependence of the ATP hydrolysis and synthesis rates. We show quantitatively how ATP hydrolysis and synthesis are both optimized and regulated given the cellular concentrations of ATP, ADP and P_i, thereby providing an answer to question 5 from the introduction.

The kinetic equations corresponding to the model shown in Figure 4 have the form

$$d[E_{1T}]/dt = k_T[E_1][T] + k_s[E_{2DP}] - (k_{-T} + k_h)[E_{1T}], \quad (4)$$

$$d[E_{2DP}]/dt = k_D[E_{2P}][D] + k_h[E_{1T}] - (k_{-D} + k_s)[E_{2DP}], \quad (5)$$

$$d[E_{2P}]/dt = k_P[P][E_2] + k_{-D}[E_{2DP}] - (k_{-P} + k_D[D])[E_{2P}], \quad (6)$$

$$d[E_1]/dt = k_{-T}[E_{1T}] + k'_h[E_2] - (k'_s + k_1[T])[E_1], \quad (7)$$

$$d[E_2]/dt = k'_s[E_1] + k_{-P}[E_2] - (k_P[P] + k'_h)[E_2], \quad (8)$$

and

$$[E_1] + [E_2] + [E_{2DP}] + [E_{1T}] + [E_{2P}] = [E_0], \quad (9)$$

where $[E_0]$ is the total concentration of the F_oF_1-ATP synthase.

The steady-state approximation is applied to Equations 4–8 corresponding to the species in Figure 4, under conditions where the frictional load is small and the reaction is heavily biased toward either ATP hydrolysis or synthesis direction such that the binding of reactants or the release of products (but not the rotation of the γ subunit) is the rate-limiting step. The inverse rate of ATP synthesis is given by

$$\frac{1}{V_{syn}} = \frac{1}{k_D[D]}\left(1 + \frac{k_{-P}}{k_P[P]}\right) + \frac{1}{k_P[P]} + \frac{1}{k_{-T}} + \frac{1}{k'_s}\frac{k_T[T]}{k_{-T}} \quad (10)$$

and that for ATP hydrolysis by

$$\frac{1}{V_{hyd}} = \frac{1}{k_T[T]} + \frac{1}{k_{-D}} + \frac{1}{k_{-P}}\left(1 + \frac{k_D[D]}{k_{-D}}\right) + \frac{1}{k'_h}\frac{k_P[P]}{k_{-P}}\left(1 + \frac{k_D[D]}{k_{-D}}\right). \quad (11)$$

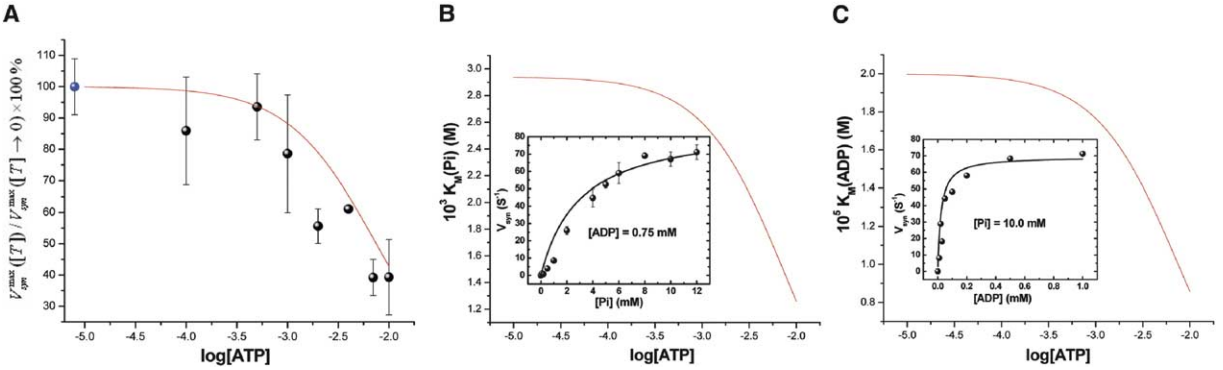

Figure 5. The Dependence of the Kinetic Parameters for ATP Synthesis upon Product Concentrations

The [ATP] concentration is in units of 1 M. Red curves show the predictions for (A) V_{syn}^{max}, (B) $K_M(P_i)$, and (C) K_M(ADP). In (A), experimental values (with error estimates) are shown; the blue spot represents the value for [ATP] equal to zero. In (B), the embedded figure shows calculated and experimental results for the rates of ATP synthesis at various P_i concentrations when the ADP concentration is 0.75 mM. In (C), the embedded figure shows calculated and experimental results for the rates of ATP synthesis at various ADP concentrations when the P_i concentration is 10.0 mM. The data were provided by R.K. Nakamoto (Al-Shawi et al., 1997).

For definitions of the symbols in Equations 10 and 11, see Figure 4 and the caption of Figure 5.

The direction and rate of the reaction are primarily determined by the magnitude of the proton-motive force. This property of the E_1E_2 mechanism is essential for an enzyme like F_oF_1-ATP synthase, which works in both directions with high efficiency. In other words, ATP and ADP/P_i do not compete for binding at the same binding site, such that the inhibition due to binding of the products to the reactant binding sites is avoided in both ATP hydrolysis and synthesis. As a result, the presence of high concentrations of ATP in the solution does not suppress ATP synthesis (see below for the inhibition constant of ATP).

Equations 10 and 11 permit one to estimate the important kinetic parameters, such as the maximum ATP synthesis rate, the Michaelis-Menten constants, K_M of the reactants (the concentration of the reactant at which the reaction rate is half of its maximum value), and the inhibition constants of the products. They are analyzed in the Supplemental Data. For example, from Equation 10, the maximum ATP synthesis rate, corresponding to [D],[P] $\rightarrow \infty$ and [T] $\rightarrow$ 0, is $k_{-T} = K_T k_T$, where K_T and k_T are the dissociation constant and the binding rate constant of ATP to the β_E site. K_T and k_T were shown to be about 25 μM and 2 × 10^6 $M^{-1}s^{-1}$ (Senior et al., 2002), and thus the maximum ATP synthesis rate is about 50 s^{-1}, consistent with the experimental values of 60–80 s^{-1} (Boyer, 1997; Senior et al., 2002). In the presence of high concentrations of P_i, Equation 10 also provides an approximate relation between the Michaelis-Menten constant K_M(ADP) for ADP and the maximum ATP synthesis rate

$$V_{syn}^{max} = K_M(ADP)k_D. \quad (12)$$

Because the maximum ATP synthesis rate is about 50 s^{-1} (as shown above) and the experimental value of K_M(ADP) is about 25 μM, the k_D is estimated to be 2 × 10^6 $M^{-1}s^{-1}$, close to the experimental value of 5 × 10^5 $M^{-1}s^{-1}$. Using a similar equation for P_i, one can determine that the P_i binding rate constant is about 2 × 10^4 $M^{-1}s^{-1}$. A 120° rotation of the γ subunit during ATP hydrolysis in the absence of the proton-motive force and under a small frictional load was shown to take about 0.2 ms (Yasuda et al., 2001). Assuming that the speed of the γ subunit is the same during the two substeps of rotation, it can be estimated that k_h' is about 1.5 × 10^4 s^{-1} (Yasuda et al., 2001; Supplemental Data). Using this value of k_h' and the binding rate constant of ADP and P_i, the inhibition of ADP and P_i on the ATP hydrolysis reaction can be estimated via Equation 11. At negligible ADP concentrations, the inhibition concentration of P_i, $K_i(P_i)$, at which the ATP hydrolysis rate is one half of its maximum value, is about 900 mM and agrees with the experimental lower limit of 10 mM obtained by Senior and coworkers (Nadanaciva et al., 1999) and also an estimated value of 10 M for *E. coli* F1-ATPase by R.K. Nakamoto and coworkers (personal communication). Similarly, at low P_i concentrations, the K_i(ADP) is shown to be 30 μM, again in agreement with the experiments (<100 μM). If a value of 1.5 × 10^4 s^{-1} is also used for the rotation of the γ subunit in the reverse direction but under conditions where there is a very large proton-motive force and the reaction is predominantly in the ATP synthesis direction, Equation 10 can be used to estimate the inhibition concentration of ATP, K_i(ATP), at which the maximum rate of ATP synthesis is one half of its value. From Equation 10, K_i(ATP) is estimated to be 7.5 mM, whereas the experimental value is 5 mM.

The calculated kinetic parameters and the available experimental results are listed in Table 1. Figure 5 shows the maximum rate of ATP synthesis and the K_M values for ADP and P_i, respectively, as a function of ATP concentration. All products (ATP in synthesis and ADP/P_i in hydrolysis) inhibit the reaction. Consequently, the higher the concentration or concentrations of the product or products, the smaller the maximum rate constant (see Figure 5 and Supplemental Data). Importantly, the K_M values of the reactants also decrease when the solution concentration of the products increases. This result is an essential property of the enzyme, which

Table 1. Kinetic Parameters

	V_{syn}^{max}	k_D	K_i (*Pi*)	K_i (*ADP*)	K_i (*ATP*)
Exp.	60–80 s^{-1}	5×10^5 $M^{-1}s^{-1}$	>10 mM	<100 μM	5 mM
Est.	50 s^{-1}	2×10^6 $M^{-1}s^{-1}$	900 mM	30 μM	7.5 mM

Maximum rate V_{syn}^{max} for ATP synthesis, ADP binding rate constant k_D, and inhibition constant K_i of P_i, ADP, and ATP. K_i (*ADP*) and K_i(*Pi*) are the concentrations of ADP and Pi when the rate of ATP hydrolysis takes one-half of its maximum value (at saturating conentrations of ATP), and K_i (*ATP*) is the concentration of ATP at which ATP synthesis takes one-half of its maximum value (at saturating concentrations of ADP and Pi). The method used to determine the parameters is described in the main text.

makes the K_M value of each ligand (ATP, ADP, and P_i; see below) low enough such that the maximum rates of both ATP hydrolysis and synthesis can be achieved.

In contrast to the E_1E_2 mechanism proposed here, competitive binding between the reactant and product at the same binding site would allow at most only one of the two reactions to achieve a maximum rate constant at any given concentrations of ligands. Such a mechanism would not serve the biological function of F_oF_1-ATP synthase, nor does it agree with the experimental observations. Experiments show that the K_M values for ADP and P_i (29 μM and 1 mM) in ATP synthesis and the K_M value for ATP (25 μM) in hydrolysis are all lower than their cellular concentrations. As discussed above (see Table 1), the present model gives inhibition concentrations for both ATP hydrolysis and synthesis that are consistent with the experimental results. From the analysis, it also follows that, at cellular conditions, only ADP plays a significant role in regulating the function of the enzyme through product inhibition, which is consistent with experimental observations (Nicholls and Ferguson, 2002). The ATP and P_i cellular concentrations are lower than their inhibition concentrations and thus are much less important. The different role of ADP from that of ATP and P_i is consistent with the fact that ADP has a concentration more than ten times lower than that of either ATP and P_i, and thus its change leads to the sensitive regulation of the enzymatic activity and has only minor influence on the concentrations of the other two.

The kinetic model leads to results that can be tested by experiments (see also Supplemental Data). It is predicted that the Michaelis-Menten constants for ADP and P_i decrease with increasing ATP concentration (as shown in Figure 5), such that $V_{syn}^{max}/K_M(Pi)$ is independent of ATP concentration at any given ADP concentration, as is $V_{syn}^{max}/K_M(ADP)$. These predicted results are consistent with the experiments of Grubmeyer et al. (1982), which showed that, for ATP synthesis, $V_{syn}^{max}/K_M(ADP)$ is a constant. The model predicts a value of about 10^4 $M^{-1}s^{-1}$ for the important binding rate constant of P_i of *E. coli* F_1-ATPase, which has not been measured. Also, the model predicts the occupancy of various sites as a function of the reactant concentrations, which are not yet known experimentally. With the recent demonstration that F_1-ATPase can synthesize ATP (Itoh et al., 2004), more data are likely to become available to provide additional tests.

Structural Basis of Thermodynamics and Kinetics (Questions 3 and 6)

Simulation studies also allow us to understand how essential residues modulate the chemical reactions in the binding sites. The sensitivity of the reaction free energy to small displacements of the large number of charged residues in the active site is one of the key features of the catalytic β subunits of F_1-ATPase. The small difference between the very similar structures of the β_{TP} and β_{DP} sites has been shown by free-energy simulations to result in a difference in the hydrolysis reaction free energy of 9 kcal/mol, with residues αArg373 and βArg189 making the most important contribution (Yang et al., 2003).

Figure 2 shows the key residues in the β_{DP} site with ATP bound. Residue αArg373, which is the only α subunit residue contributing to the β subunit catalytic site, has been suggested (Senior et al., 2002; Menz et al., 2001; Dittrich et al., 2004) to play a role in F_1-ATPase hydrolysis analogous to the so-called "arginine finger" in GTPases (Rittinger et al., 1997). Structural studies have shown that αArg373 can be at a distance of 10 Å from the phosphate in the β_{TP} site (Gibbons et al., 2000, Kagawa et al., 2004), in contrast to its position in other structures (Abrahams et al., 1994; Braig et al., 2000; Menz et al., 2001). Also, if αArg373 is mutated, hydrolysis is slowed down significantly and synthesis is eliminated (Senior et al., 2002). Calculations of ATP unbinding from the catalytic site confirm that αArg373 moves away when ATP is no longer present and that αArg373 is essential for biasing the reaction free energy in the direction of hydrolysis and at the same time lowers the activation barrier (Yang et al., 2003; W.Y., Y.Q.G., S. Boresch, and M.K., unpublished data). Conversely, a displacement of αArg373 from the active site by a conformational change due to rotation of the γ subunit (from β_{TP} to β_{TP}*, as suggested in Figure 3A) shifts the thermodynamic potential so as to favor ATP synthesis. Residue βArg189, whose equivalent is not present in GTPases, has been found to be important for ATP synthesis (Boyer, 1997; Senior et al., 2002). Overall, the Arg pair (αArg373 and βArg189) and their relative positioning appear to make the major contribution to switching between hydrolysis and synthesis. Structural studies (Kagawa et al., 2004) and simulations suggest that αArg373 acts to "transmit conformational signals across the α/β subunit catalytic interface" (Nadanaciva et al., 1999) as part of the chemomechanical coupling to the γ subunit. Calculations indicate that in a model for β_{TP}*, residue βGlu188 is in approximately the same position relative to the ATP γ-phosphate group as in the β_{TP} structures (Abrahams et al., 1994, Menz et al., 2001). It can polarize the water molecule that is involved in the synthesis reaction in β_{TP}* and in the hydrolysis reaction in β_{DP}. Together with βGlu188, other residues such as βLys162 are essential for the catalysis of synthesis and

hydrolysis. Small displacements of these residues can significantly change the reaction rate. For instance, during ATP synthesis, after the formation of ATP at the β_{TP}* site, the displacements of catalytic residues appear to prevent ATP with high chemical potential from being hydrolyzed to ADP/P_i, suggesting kinetic rather thermodynamic control. The mutation of charged residues not in direct contact with the ligand, such as βArg246, has been shown recently to lead to the loss of activity (Ahmad and Senior, 2004). This is indicative of the intricacy of the structure of the catalytic region of the β subunits, which is required to fulfill the multiple functions of regulating absolute binding, relative binding, chemical catalysis, and conformational change.

Conclusion

A detailed mechanism for ATP synthesis and hydrolysis has been proposed on the basis of molecular dynamics simulations; kinetic modeling; and experimental structural, thermodynamic, and kinetic data. The model, which represents the first consistent description of how this bifunctional enzyme is able to perform both ATP synthesis and ATP hydrolysis, requires further tests. We hope that publication of the model will stimulate experimental work, as well as additional theoretical studies, to substantiate or refine the present proposal.

Supplemental Data

Supplemental Data include supplemental text, Supplemental References, and one figure and can be found with this article online at http://www.cell.com/cgi/content/full/123/2/195/DC1/.

Acknowledgments

We thank J.E. Walker for providing a preprint of Menz et al. (2001) prior to publication, R.K. Nakamoto and M.K. Al-Shawi for supplying the experimental data shown in Figure 5B, and A.E. Senior for the permission to use Figure 1. We thank J. Kuriyan for his many suggestions, which considerably improved the manuscript, and R.K. Nakamoto and A. Horwich for their comments. During development of the present model, we have learned much about this wonderful enzyme from A.G.W. Leslie, A.E. Senior, and J.E. Walker.

References

Abrahams, J.P., Leslie, A.G.W., Lutter, R., and Walker, J.E. (1994). Structure at 2.8 resolution of F1-ATPase from bovine heart mitochondria. Nature *370*, 621–628.

Ahmad, Z., and Senior, A.E. (2004). Mutagenesis of residue betaArg-246 in the phosphate-binding subdomain of catalytic sites of Escherichia coli F1-ATPase. J. Biol. Chem. *279*, 31505–31513.

Alberts, B. (1998). The cell as a collection of protein machines: preparing the next generation of molecular biologists. Cell *92*, 291–294.

Allison, W.S. (1998). F_1-ATPase: A molecular motor that hydrolyzes ATP with sequential opening and closing of catalytic sites coupled to rotation of its γ-subunit. Acc. Chem. Res. *31*, 819–826.

Al-Shawi, M.K., Ketchum, C.J., and Nakamoto, R.K. (1997). Energy coupling, turnover, and stability of the F0F1 ATP synthase are dependent on the energy of interaction between gamma and beta subunits. Biochemistry *36*, 12961–12969.

Antes, I., Chandler, D., Wang, H.Y., and Oster, G. (2003). The unbinding of ATP from F1-ATPase. Biophys. J. *85*, 695–706.

Böckmann, R.A., and Grubmüller, H. (2002). Nanoseconds molecular dynamics simulation of primary mechanical energy transfer steps in F1-ATP synthase. Nat. Struct. Biol. *9*, 198–202.

Boyer, P.D. (1993). The binding change mechanism for ATP synthase—some probabilities and possibilities. Biochim. Biophys. Acta *1140*, 215–250.

Boyer, P.D. (1997). The ATP synthase—a splendid molecular machine. Annu. Rev. Biochem. *66*, 717–749.

Braig, K., Menz, R.I., Montgomery, M.G., Leslie, A.G.W., and Walker, J.E. (2000). Structure of bovine mitochondrial F(1)-ATPase inhibited by Mg(2+) ADP and aluminium fluoride. Struct. Fold. Des. *8*, 567–573.

Cui, Q., Li, G., Ma, J., and Karplus, M. (2004). A normal mode analysis of structural plasticity in the biomolecular motor F(1)-ATPase. J. Mol. Biol. *340*, 345–372.

DeMeis, L., and Vianna, A.L. (1979). Energy interconversion by the Ca2+-dependent ATPase of the sarcoplasmic reticulum. Annu. Rev. Biochem. *48*, 275–292.

Diez, M., Zimmermann, B., Borsch, M., Konig, M., Schweinberger, E., Steigmiller, S., Reuter, R., Felekyan, S., Kudryavtsev, V., Seidel, C.A.M., and Graber, P. (2004). Proton-powered subunit rotation in single membrane-bound F0F1-ATP synthase. Nat. Struct. Biol. *11*, 135–141.

Dittrich, M., Hayashi, S., and Schulten, K. (2004). ATP hydrolysis in the betaTP and betaDP catalytic sites of F1-ATPase. Biophys. J. *87*, 2954–2967.

Gao, Y., Yang, W., Marcus, R.A., and Karplus, M. (2003). A model for the cooperative free energy transduction and kinetics of ATP hydrolysis by F1-ATPase. Proc. Natl. Acad. Sci. USA *100*, 11339–11344.

Gibbons, C., Montgomery, M.G., Leslie, A.G.W., and Walker, J.E. (2000). The structure of the central stalk in bovine F(1)-ATPase at 2.4 A resolution. Nat. Struct. Biol. *7*, 1055–1061.

Greene, M.D., and Frasch, W.D. (2003). Interactions among gamma R268, gamma Q269, and the beta subunit catch loop of Escherichia coli F1-ATPase are important for catalytic activity. J. Biol. Chem. *278*, 51594–51598.

Grubmeyer, C., Cross, R.L., and Penefsky, H.S. (1982). Mechanism of ATP hydrolysis by beef heart mitochondrial ATPase. Rate constants for elementary steps in catalysis at a single site. J. Biol. Chem. *257*, 12092–12100.

Itoh, H., Takahashi, A., Adachi, K., Noji, H., Yasuda, R., Yoshida, M., and Kinosita, K., Jr. (2004). Mechanically driven ATP synthesis by F1-ATPase. Nature *427*, 465–468.

Kagawa, R., Montgomery, M.G., Braig, K., Leslie, A.G.W., and Walker, J.E. (2004). The structure of bovine F1-ATPase inhibited by ADP and beryllium fluoride. EMBO J. *23*, 2734–2744.

Karplus, M., and Gao, Y.Q. (2004). Biomolecular motors: the F1-ATPase paradigm. Curr. Opin. Struct. Biol. *14*, 250–259.

Kinosita, K., Jr., Adachi, K., and Itoh, H. (2004). Rotation of F1-ATPase: how an ATP-driven molecular machine may work. Annu. Rev. Biophys. Biomol. Struct. *33*, 245–268.

Ma, J., Flynn, T.C., Cui, Q., Leslie, A.G.W., Walker, J.E., and Karplus, M. (2002). A dynamic analysis of the rotation mechanism for conformational change in F(1)-ATPase. Structure (Camb.) *10*, 921–931.

Menz, R.I., Walker, J.E., and Leslie, A.G.W. (2001). Structure of bovine mitochondrial F(1)-ATPase with nucleotide bound to all three catalytic sites: implications for the mechanism of rotary catalysis. Cell *106*, 331–341.

Nadanaciva, S., Weber, J., Wilke-Mounts, S., and Senior, A.E. (1999). Importance of F1-ATPase residue alpha-Arg-376 for catalytic transition state stabilization. Biochemistry *38*, 15493–15499.

Nakamoto, R.K., Ketchum, C.J., Kuo, P., Peskova, Y.B., and Al-Shawi, M.K. (2000). Molecular mechanisms of rotational catalysis in the F(0)F(1) ATP synthase. Biochim. Biophys. Acta *1458*, 289–299.

Nelson, D.L., and Cox, M.M. (2000). In Lehninger Principles of Biochemistry, Third Edition (New York: Worth Publishers).

Nicholls, D., and Ferguson, S.J. (2002). In Bioenergetics *3* (Amsterdam: Academic Press).

Noji, H., Yasuda, R., Yoshida, M., Kinosita, K., and Itoh, H. (1997). Direct observation of the rotation of F1-ATPase. Nature *386*, 299–302.

Rastogi, V.K., and Girvin, M.E. (1999). Structural changes linked to proton translocation by subunit c of the ATP synthase. Nature *402*, 263–268.

Rittinger, K., Walker, P.A., Eccleston, J.F., Nurmahomed, K., Owen, D., Laue, E., Gamblin, S.J., and Smerdon, S.J. (1997). Structure at 1.65 A of RhoA and its GTPase-activating protein in complex with a transition-state analogue. Nature *388*, 693–697.

Senior, A.E. (1992). Catalytic sites of Escherichia coli F1-ATPase. J. Bioeneg. Biomem. *24*, 479–483.

Senior, A.E., Nadanaciva, S., and Weber, J. (2002). The molecular mechanism of ATP synthesis by F1F0-ATP synthase. Biochim. Biophys. Acta *1553*, 188–211.

Simonson, T., Archontis, G., and Karplus, M. (2002). Free energy simulations come of age: protein-ligand recognition. Acc. Chem. Res. *35*, 430–437.

Stryer, L. (1995). In Biochemistry (New YOrk: W.H. Freeman and Company).

Sun, S., Chandler, D., Dinner, A.R., and Oster, G. (2003). Elastic energy storage in beta-sheets with application to F1-ATPase. Eur. Biophys. J. *32*, 676–683.

Voet, D., and Voet, J.G. (1995). Biochemistry, Second Edition (New York: John Wiley), p. 433.

Wang, H., and Oster, G. (1998). Energy transduction in the F1 motor of ATP synthase. Nature *396*, 279–282.

Weber, J., and Senior, A.E. (1997). Catalytic mechanism of F1-ATPase. Biochim. Biophys. Acta *1319*, 19–58.

Yagi, H., Tsujimoto, T., Yamazaki, T., Yoshida, M., and Akutsu, H. (2004). Conformational change of H+-ATPase beta monomer revealed on segmental isotope labeling NMR spectroscopy. J. Am. Chem. Soc. *126*, 16632–16638.

Yang, W., Gao, Y.Q., Cui, Q., Ma, J., and Karplus, M. (2003). The missing link between thermodynamics and structure in F1-ATPase. Proc. Natl. Acad. Sci. USA *100*, 874–879.

Yang, W., Bitetti-Putzer, R., and Karplus, M. (2004). Free energy simulations: use of reverse cumulative averaging to determine the equilibrated region and the time required for convergence. J. Chem. Phys. *120*, 2618–2628.

Yasuda, R., Noji, H., Kinosita, K., and Yoshida, M. (1998). F1-ATPase: a rotary motor made of a single molecule. Cell *93*, 1117–1124.

Yasuda, R., Noji, H., Yoshida, M., Kinosita, K., and Itoh, H. (2001). Resolution of distinct rotational substeps by submillisecond kinetic analysis of F1-ATPase. Nature *410*, 898–904.